RESEARCH PAPER

Green arbutin-chitosan nanoparticles gel as an eco-friendly and promising product for skin lightening: *in vitro* and *in vivo* assessment

Mahmoud Omidi[1,2], Majid Saeedi[3], Mohammad Amin Zahiri[4], Saeed Azimi[1,5], Esmaeil Mohammadian [6,7*], Seyyed Mohammad Hassan Hashemi[1,8*]

[1] Food Health Research Center, Hormozgan University of Medical Sciences, Bandar Abbas, Iran
[2] Department of Pharmacology and Toxicology, Faculty of Pharmacy, Hormozgan University of Medical Sciences, Bandar Abbas, Iran
[3]Department of Pharmaceutics, Faculty of Pharmacy, Mazandaran University of Medical Sciences, Sari, Iran
[4]Student Research Committee, Faculty of Pharmacy, Hormozgan University of Medical Sciences, Bandar Abbas, Iran
[5] Department of Clinical Pharmacy, Faculty of Pharmacy, Hormozgan University of Medical Sciences, Bandar Abbas, Iran
[6]Cellular and Molecular Research Center, Research Institute for Health Development, Kurdistan University of Medical Sciences, Sanandaj, Iran
[7]Department of Medicinal Chemistry, School of Pharmacy and Pharmaceutical Sciences, Hormozgan University of Medical Sciences, Bandar Abbas, Iran
[8] Department of Pharmaceutics, Faculty of Pharmacy, Hormozgan University of Medical Sciences, Bandar Abbas, Iran

ABSTRACT

Objective(s): In the present study, a cross-linking gelation method combined with ultrasound was employed to create arbutin (ARB)-incorporated chitosan (CHT) nanoparticles (NPs). This approach aims to enhance cutaneous absorption and improve anti-melanogenesis effects.

Material and Methods: Environmentally-friendly preparation of NP, monitoring NP features, checking structure, animal safety application, cellular viability, and inhibitory assessment on melanin creation were performed.

Results: The results showed that increasing the volume ratio of chitosan (CHT) to tripolyphosphate (TPP) from 10:1.25 to 10:5 resulted in a reduction of particle size from 1097.133 ± 28.655 nm to 215.666 ± 5.976 nm. Moreover, this CHT/TPP volume ratio increase from 10:1.25 to 10:5 enhanced the encapsulation efficiency, from 55.084 ± 4.283% to 97.151 ± 0.066%. Assessment of cutaneous absorption revealed that the ARB-CHT-NP gel delivered significantly more arbutin (ARB) to both the cutaneous layers (46.168 ± 3.313% or 810.094 ± 58.147 µg/cm²) and the receiver compartment (34.155 ± 2.699% or 599.314 ± 47.371 µg/cm²) compared to the ARB plain gel. In vitro cytotoxicity testing demonstrated that, in the presence of the optimal formulation, a higher percentage of cell survival was observed in the HFF cell line compared to kojic acid and ARB. Additionally, the ARB-CHT-NP gel exhibited greater cytotoxicity in the B16F10 cell line compared to the other groups. A cutaneous itching assay on Wistar rats showed no signs of sensitivity to the ARB-CHT-NP gel. Furthermore, ARB-CHT-NP inhibited melanogenesis more effectively than kojic acid and ARB. L-dopa auto-oxidation was also significantly inhibited by ARB-CHT-NP (56.971 ± 1.265%) compared to kojic acid (46.141 ± 1.169%) and ARB (41.308 ± 1.967%).

Conclusion: Based on the results, the ARB-CHT-NP could serve as a prospective nanocarrier for ARB cutaneous application. Therefore, it is recommended that its use for treating melasma be considered.

Keywords: *Arbutin, Chitosan, Nanoparticle, Anti-melanogenesis, Environmentally friendly preparation*

How to cite this article
Omidi M, Saeedi M, Zahiri MA, Azimi S, Mohammadian E, Hashemi SMH. Green arbutin-chitosan nanoparticles gel as an eco-friendly and promising product for skin lightening: in vitro and in vivo assessment. Nanomed J. 2026; 13(1): 224-237. DOI: 10.22038/NMJ.2025.83053.2075

* *Corresponding author(s):* Seyyed Mohammad Hassan Hashemi, Assistant Professor, Food Health Research Center, Hormozgan University of Medical Sciences, Bandar Abbas, Iran. E-mail: *smhhashemipharma@gmail.com*. Esmaeil Mohammadian, Assistant Professor, Cellular and Molecular Research Center, Research Institute for Health Development, Kurdistan University of Medical Sciences, Sanandaj, Iran. E-mail:*e.mohamadyan1390@gmail.com*.

Note. This manuscript was submitted on October 18, 2024; approved on December 21, 2024.

GRAPHICAL ABSTRACT

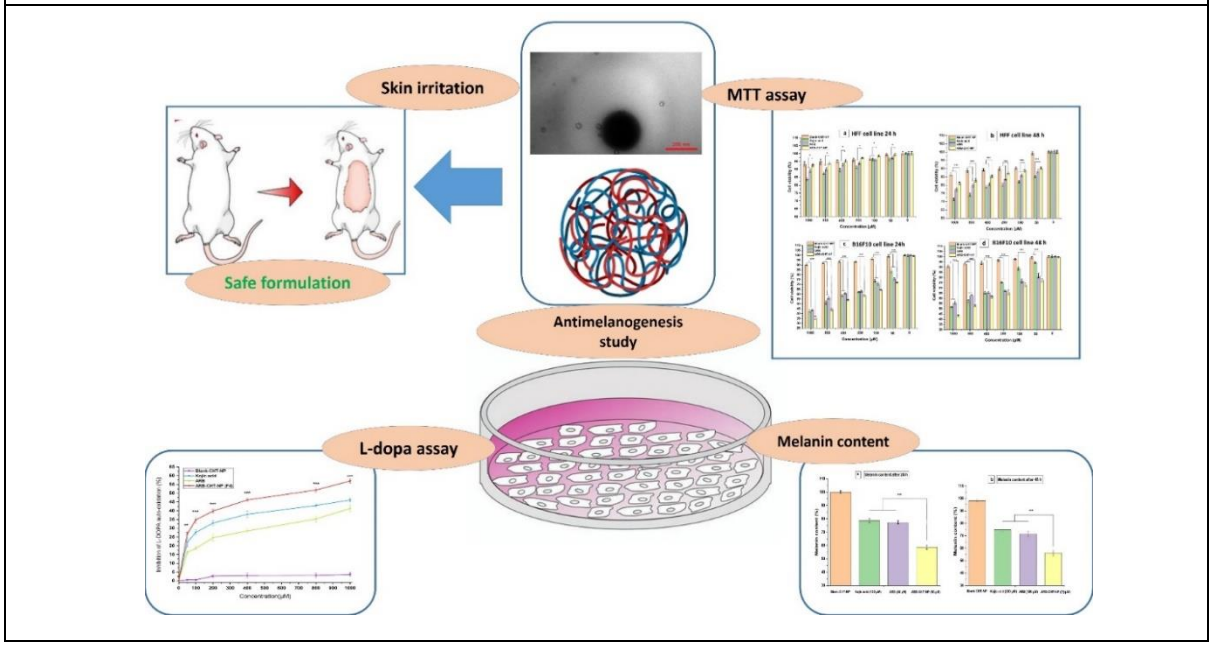

INTRODUCTION

Dermatological conditions can significantly impact an individual's physical appearance, affecting self-perception, psychosocial development, and interpersonal dynamics. These factors often lead to increased anxiety and psychological consequences [1]. Approximately 33% of individuals presenting to dermatology clinics are also affected by psychiatric conditions, suggesting a potential for comorbidities [2]. The quality of life is an important consideration when developing new therapeutic regimens and formulations, as a person's overall health is influenced by factors beyond the pathological condition [2]. Melasma is a facial pigmentation disorder that primarily affects the cheeks, forehead, and upper lip. This condition predominantly affects women, with a prevalence of approximately 90% [3]. The prevalence of melasma varies globally and is influenced by various factors. While its overall prevalence in the general population is around 1%, it ranges between 9% and 50% in high-risk groups. In addition, melasma has a significant negative impact on individuals' social lives, leading to issues such as social isolation and anxiety [4]. Hydroquinone, kojic acid, and azelaic acid are commonly used skin-lightening agents that suppress melanin production and are employed to treat hyperpigmentation. However, melasma treatments often have various side effects [5]. In recent years, growing interest has been in identifying compounds that inhibit melanogenesis to enhance food quality and improve human health. This is particularly evident in Eastern cultures, where skin lighteners are highly sought after [6]. Furthermore, the pharmaceutical industry has shown increased attention to natural compounds, as plant extracts are a significant source of bioactive substances. Historically, herbal products have been used in medicine and cosmetics for various health benefits [6]. Arbutin (ARB), a derivative of hydroquinone found in plants such as cranberry, pear, and bearberry, inhibits tyrosinase, the key enzyme in melanin production. ARB is widely used as a skin-lightening agent in cosmetics, particularly across Asia. Studies have demonstrated that ARB and its derivatives can inhibit tyrosinase activity both in vitro and in vivo [7-11]. In a controlled, randomized pilot study, all patients showed clinical improvement using 1% w/w ARB [10]. Another study indicated that 7% w/w ARB and laser therapy effectively treated stubborn melasma [11]. These findings show ARB is incorporated into various cosmeceutical products in the US, Japan, and Korea [12]. However, the use of ARB in topical products is limited due to its insufficient cutaneous diffusion and storage instability [13].

Several challenges are associated with the delivery of hydrophilic materials, such as arbutin (ARB). Therefore, the development of new formulations for these hydrophilic substances is of particular importance [14]. The main challenges include (a) low absorption and inadequate biodistribution across biological membranes, (b) low bioavailability, and (c) a short half-life in the systemic circulation. To overcome these limitations,

nano-carriers loaded with hydrophilic pharmaceuticals have been introduced [15].

Nanotechnology has recently gained significant attention in cosmetics and pharmaceuticals due to its unique benefits[16]. In particular, using chitosan in nanoparticle formulations has garnered interest in these fields. It has been reported that chitosan nanoparticles (CHT-NP) have been utilized for dermal drug delivery in malignant melanoma [17]. CHT-NPs are considered suitable for drug delivery because they are biodegradable, non-toxic, and risk-free [18]. Additionally, CHT-NPs possess a robust polymeric matrix that facilitates prolonged drug release [19]. Several studies have demonstrated that CHT-NPs can penetrate all layers of the skin [20]. Another study showed that, when used topically, the CHT/collagen polymeric-NP gel product achieved a skin depot equivalent to a plain gel [21].

Using chitosan nanoparticles (CHT-NP) as a vehicle for the local delivery of arbutin (ARB) is of considerable interest, particularly when environmentally friendly methods, such as ultrasonication and ionic gelation, are employed. Moreover, the dermatological sensitivity potential of CHT-NP gel formulations containing ARB has not been thoroughly reviewed. While the properties of ARB-CHT-NP have not been extensively studied in terms of cell viability in previous research, the investigation of its inhibitory effects on melanin formation and L-DOPA auto-oxidation represents one of the strengths of the present study. In conclusion, ARB-CHT-NP offers a promising alternative to traditional carriers when used in cosmeceutical products.

MATERIALS AND METHODS

Materials

Arbutin (ARB) (catalog number: A4256-10G) and RPMI medium were obtained from Sigma-Aldrich (Germany). Chitosan (pharmaceutical grade, medium molecular weight with a deacetylation degree >75% and a molecular weight of 190,000 Da) was purchased from Merck (Germany). Fetal bovine serum (FBS) and DMEM medium were obtained from Gibco (USA). Hydroxypropyl methylcellulose (HPMC) K100M was obtained from Sigma-Aldrich (Germany).

Preparation of ARB-CHT- NP

Calvo et al. outlined a method for fabricating chitosan (CHT)/tripolyphosphate (TPP) nanoparticles (NPs) based on the cross-linking gelation of CHT with TPP anions and ultrasonication [22]. The preparation method for ARB-CHT-NPs was adapted from this study. A 0.25% w/v CHT solution was prepared by dissolving 50 mg of CHT in 20 mL of 1% v/v acetic acid at 25 °C for 3 hours with stirring. A 2 mg/mL TPP solution was prepared by dissolving the required amount of TPP in 20 mL of deionized water. Thus, 200 mg of arbutin (ARB) was added to the CHT solution. Different volumes of the TPP solution were then added to the CHT solution (0.25% w/v) and thoroughly mixed for 1 hour under moderate stirring (1000 rpm). ARB-CHT/TPP nanoparticles were obtained at this stage (Table 1). The resulting compound was then sonicated for 10 minutes using probe sonication (Bandelin; 3100; Germany) at 100% amplitude.

Formulating ARB-CHT- NP Gel and ARB Simple Gel

To formulate the nanoparticle (NP) gel, HPMC K100M (1.5% w/w) was dissolved in an aqueous solution containing ARB-CHT-NP (including 200 mg of ARB) and left to stand overnight with bacteriostatic treatment. Next, the mixture was blended in a propeller blender at 500 rpm. An ARB solution (including 200 mg of ARB) was combined with HPMC K100M and blended at 500 rpm to prepare the ARB-simple gel.

Nanoparticle characterization

The average radius, polydispersity index (PDI), and zeta potential (ZP) of the nanoparticles (NPs) were measured using a Zetasizer Nano-ZS device and dynamic light scattering (DLS) from Malvern Instruments Ltd., UK. The interaction between the components was evaluated with a Cary 630 FTIR spectrophotometer (Agilent Technologies Inc., CA, USA), equipped with a diamond ATR (attenuated total reflectance). Spectra in the 4000–650 cm^{-1} range with a resolution of 2 cm^{-1} were obtained. Differential scanning calorimetry (DSC) analysis was performed using a Pyris-6 instrument from PerkinElmer (Norwalk, USA). Additionally, the morphological properties and structural characteristics of the NPs were examined by transmission electron microscopy (TEM) using a Philips EM 208S.

EE% determination

The drug incorporation was evaluated by centrifuging the ARB-CHT-NP at 13,000 rpm for 30 minutes using a 3–15 kS Sigma centrifuge (Germany). The supernatant was then filtered through a 0.22 µm pore size filter. The absorbance of the resulting liquid phase was measured using a UV-Vis spectrophotometer at 294 nm. The amount of ARB in the clarified solution was quantified based on the absorbance readings. The encapsulation efficiency (EE%) of the nanoparticles (NPs) was calculated using the following equation.

$$EE\% = \frac{Winitial - Wfree}{Winitial} \times 100$$

Drug release

The pharmaceutical release assay used immersion cells with cellulose acetate membranes (MWCO 12 kDa) [19, 23]. A 200 mg/30 mL concentration was utilized to prepare the ideal gel. A 5-gram portion of this product was set aside, and an assay test was conducted before placing it in the immersion cell (the amount corresponding to 5 grams of gel is 33 mg). The cells were then exposed to 5 g of gel containing 33 mg of ARB. Subsequently, the cells were sealed with a cap after being covered with a cellulose acetate membrane. The cells were placed into the USP dissolution apparatus II, with each vessel containing 450 mL of water to reduce the volume of dissolution media. The apparatus was operated at 37°C and 100 rpm. At various time points (2, 4, 6, 8, and 24 hours), 5 mL of the dissolution medium was sampled and filtered through a 0.22 µm filter. The concentration of ARB in the collected solution was determined using a UV spectrophotometer at 294 nm. A standard calibration curve, ranging from 15 to 200 µg/mL with an R^2 value of 0.999, was used to quantify the pharmaceutical content. After each sampling, 5 mL of water was added to the dissolution medium to maintain a consistent volume.

Cutaneous absorption examination

Male Wistar rats (weight: 130–160 g) were sedated with 100 µL of a ketamine/xylazine mixture. Their abdominal skin was then carefully shaved. After 48 hours, the rats were euthanized using inhalation of chloroform, and their abdominal regions were carefully excised. For the cutaneous absorption assay, the skin was meticulously cleared of adhering subcutaneous fat and soaked in normal saline at 4°C for 24 hours. The skin samples were placed into Franz cells with a diffusional area of 3.8 cm^2. The dermal layer of the skin, in direct contact with the medium (receiver part), was used for the experiment. Pure water was used to saturate the receiver part, and the diffusion cells were maintained at 32 ± 0.5°C with stirring at 150 rpm. In the next step, 1 g of ARB-CHT-NP gel (0.6% w/w) and 1 g of ARB gel (0.6% w/w) (as a control) were homogenously applied to the donor section. At 2, 4, 6, 8, and 24 hours, 5 mL of solution was removed from the receptor phase, with the volume maintained constant by adding 5 mL of fresh medium. The drug concentration in the collected solutions was determined using a UV-visible spectrophotometer at 294 nm.

Cutaneous retaining inspections

After completing the cutaneous absorption assay, the skin samples were washed three times with fresh aqueous solution and dried to determine the residual ARB content. The removed skin was finely minced and transferred to a tube. In the next step, the tissue was digested in aqueous media and subsequently sonicated in an ultrasonic bath for 1 hour. At the end of the test, the solution was double-filtered using a syringe filter with a pore size of 0.22 µm and analyzed using a UV-VIS spectrophotometer at 294 nm.

Cellular survival assessment

In this study, the cytotoxicity of all treatment groups was assessed using the HFF and B16F10 cell lines obtained from the Pasteur Institute (Tehran, Iran). Initially, 5000 cells were seeded into 96-well microplates and incubated for 24 hours with varying concentrations (1000, 800, 400, 200, 100, and 50 µM) of ARB-CHT-NP, CHT-NP without ARB, and kojic acid. The samples were then incubated for either 24 or 48 hours. Following incubation, the cells were washed with PBS to remove residual substances. Cell survival was determined by evaluating formazan formation using the MTT assay. The cells were incubated with MTT solution (0.5 mg/mL) at 37°C for 4 hours. After incubation, the formazan crystals were dissolved in 100 µL of DMSO. The plates were then shaken for 20 minutes, and the optical density (OD) was measured at 560 nm using a multi-well spectrophotometer. Several concentrations ranging from 50 to 1000 µM were tested in triplicate, with six additional control samples. Cell viability was then calculated using the following formula:

Cell safety%= [OD560 (sample)/OD560 (control)] × 100

Melanin content evaluation

To calculate melanin content, B16F10 cells were seeded at a 5 × 10^4 cells/well density in 12-well plates. DMEM medium was supplemented with 10% (v/v) fetal bovine serum (FBS) and 1% (v/v) Penicillin/Streptomycin. The cells were incubated for 24 and 48 hours at 37°C with 5% CO_2 and 85% humidity. After incubation, the cells were treated with the appropriate concentration of ARB solution (IC_{50} concentration from the MTT assay on B16F10 cells) and optimum ARB-CHT-NP and kojic acid concentrations. The cells were incubated for an additional 24 and 48 hours. Afterward, the cell pellets were treated with 100 µL of 2 M NaOH solution and heated at 100°C for 30 minutes. The melanin content in all groups was measured by absorbance at 405 nm using a microplate reader (BioTek, Winooski, USA).

Table 1. Ingredients and physico-chemical properties of product. The records involves of the mean ±SD (n=3)

Formulation	ARB (mg)3	CHT [a] (mg)	TPP [b] (mg/mL)	CHT/TPP volume ratio	Particle size nm	PDI [c]	Zeta potential (mv)	EE [d] (%)
F1	200	50	2	10:1.25	1097.133± 28.655	0.627±0.013	24.433± 1.137	55.084± 4.283
F2	200	50	2	10: 2.5	823.400± 19.382	0.494±0.009	20.300± 1.081	63.635± 2.474
F3	200	50	2	10: 3.75	434.933± 11.019	0.333±0.008	15.800± 0.984	84.708± 1.884
F4	200	50	2	10:5	215.666± 5.976	0.209±0.007	11.466± 0.986	97.151± 0.066

Inhibitory L-DOPA auto-oxidation test

The inhibitory properties of L-DOPA auto-oxidation were evaluated using concentrations of 1000, 800, 400, 200, 100, and 50 µM of ARB, kojic acid, and ARB-CHT-NP. Briefly, 10 mM L-DOPA (in 0.1 mM potassium phosphate buffer, pH 6.5) was mixed with various concentrations of the samples (in 0.1 M sodium phosphate buffer, pH 6.5) to a total volume of 300 µL. After incubating at 30°C for 15 minutes, inhibitory activity was assessed by measuring the optical density at 475 nm [24].

In vivo skin safety assessments of the products

Animals

These trials used male Wistar rats weighing 130 and 200 g in groups of nine in acrylic cages within a controlled animal facility. The rats were maintained under a 12-hour light/dark cycle, with lights on from 07:00 to 19:00 h, at 21 ± 2°C. It is important to note that food was continuously available to the rats, except during the trial periods. Additionally, each rat was used only once.

Dermal itching trial

This study investigated the potential sensitization effects of topical treatments under institutional animal ethics guidelines. Male Wistar rats were divided into five groups (n = 6 per group) for this purpose:

1. **Control:** Received no treatment.
2. **Group II:** Treated with ARB-CHT-NP gel.
3. **Group III:** Treated with ARB-plain gel.
4. **Group IV:** Treated with blank-NP gel.
5. **Group V:** Treated with a standard sensitizing agent (0.8% formalin solution).

Each group received its assigned treatment daily for seven days. A standardized rating system was used to visually assess the treated areas throughout the study [25].

Statistic assessment

This study used ANOVA followed by Tukey's post-hoc test to assess the identified factors. All values are presented as mean ± SD. Statistical analyses were performed using SPSS 22.0 (IBM Co., USA). Additionally, the t-test was employed to compare significant changes in cutaneous absorption. A p-value of < 0.05 was considered statistically significant.

RESULTS AND DISCUSSION

Analysis of ARB-CHT-NP

Crosslinking gelation and ultrasound methods were used to develop ARB-loaded CHT-NP. Different amounts of CHT were combined with varying fractions of TPP (10:1.25, 10:2.5, 10:3.75, and 10:5 v/v) to achieve the optimal properties of ARB-CHT-NP.

Table 1 presents the composition and characteristics of the synthesized nanoparticles. As shown, increasing the CHT/TPP ratio from 10:1.25 (F1) to 10:5 (F4) resulted in a significant reduction in nanoparticle diameter, from 1097.133 ± 28.655 nm to 215.6667 ± 5.976 nm ($P < 0.001$). This decrease in nanoparticle size can be attributed to the higher availability of TPP for cross-linking with CHT. The increased TPP concentration promotes a higher degree of internal cross-linking within the NP structure, leading to the formation of smaller particles [26]. A similar trend has been observed in previous studies; research by Hejjaji et al. and Shah et al. demonstrated that increasing the CHT/TPP ratio reduced CHT-NP diameter. These studies highlight the critical role of the CHT/TPP ratio in determining NP size [18, 27].

The PDI values ranged from 0 to 1, with lower values indicating a monodisperse distribution of particles in the suspension [28]. As shown in Table 1, the PDI values ranged from 0.209 ± 0.007 to 0.627 ± 0.013 ($P < 0.01$). These results suggest that increasing the CHT/TPP ratio led to a more monodisperse particle distribution. It can be concluded that a higher CHT/TPP ratio promotes the formation of nanoparticle populations with more uniform size distributions. It should be noted that various parameters, such as the type of CHT, its molecular weight, sonication power, crosslinking efficiency, and surface charge, can influence the reduction of PDI values. Furthermore, CHT can act as a template or nucleation site for nanoparticle formation, affecting the uniformity of particle nucleation and growth. CHT creates a consistent environment for nucleation and growth, which helps produce nanoparticles with a more uniform size distribution and lower PDI. According to the

thermodynamic scaling effect in forming ionic gelation particles, reducing the polymeric matrix radius leads to a narrower normalized distribution. Additionally, increasing the CHT/TPP ratio can influence the degree of crosslinking and the size distribution of the nanoparticles [29, 30]. These observed trends are consistent with previous research [19, 31].

Table 1 presents the encapsulation efficiency (EE%) of arbutin (ARB) for each NP formulation. The data show that ARB encapsulation efficiency increased significantly, ranging from 55.084 ± 4.283% to 97.151 ± 0.066%. This observed increase in EE% with the increasing CHT/TPP volume fraction can be attributed to the influence of polyanions on inter- and intramolecular cross-linking. Under acidic conditions, the positive charge of the quaternary amine groups in CHT interacts with the polyanionic TPP, leading to enhanced gelation and, consequently, higher ARB encapsulation. NP formation occurs through the rapid mixing of TPP and CHT solutions. Additionally, the resulting EE% is significantly affected by both the CHT/TPP ratio and the pH. The positive charge of CHT plays a crucial role in NP formation due to electrostatic interactions with negatively charged substances (pH 5). In addition to the electrostatic interactions between TPP and CHT, hydrogen bonds formed among TPP, CHT, and ARB molecules during NP formation further enhance EE%. The increased viscosity of the CHT/TPP fractions can lead to a reduction in EE% and an increase in NP diameter. Previous studies have shown that increasing the CHT/TPP ratio also led to a rise in EE% in venlafaxine-CHT-NP formulations [18, 19].

Table 1 also shows that increasing the CHT/TPP ratio decreased the zeta potential (ZP) of the nanoparticles (NPs). Notably, at the lower CHT/TPP ratio (10:1.25), the zeta potential was measured at 24.43 mV. However, as the CHT/TPP ratio increased to 10:5, the ZP decreased to 11.46 mV. Furthermore, a decrease in encapsulation efficiency (EE%) related to ARB was observed with increasing zeta potential. This phenomenon can be attributed to the dispersion of unbound ARB and CHT in the liquid phase, as well as the formation of a diffusion layer, hydrogen bonding, and electrostatic interactions between TPP and CHT during the formation of CHT-NP [18, 32].

It is well known that the ideal nanoparticle (NP) should have a small particle size, a low polydispersity index (PDI), and high encapsulation efficiency (EE%). However, achieving nanoparticles with these optimal properties is challenging. In this study, ARB-CHT-NP formulation 4 (F4) was selected for further investigation due to its exceptional characteristics, including a minimal NP diameter (215.666 ± 5.976 nm), the highest encapsulation efficiency (97.151 ± 0.066%), and a PDI of 0.209 ± 0.007.

TEM assessment

Morphology is one of the most important physical and chemical properties of nanoparticles. The morphology of ARB-CHT-NP formulation 4 (F4) was investigated (Figure 1). The results showed that the nanoparticles are spherical, with a size of approximately 250 nm. It is important to note that the nanoparticle size was determined using both TEM and DLS techniques, and the results from both methods were consistent.

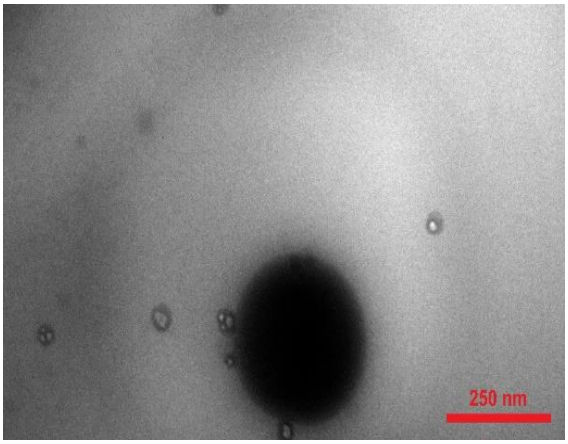

Fig. 1. TEM image of optimum formulation (ARB-CHT-NP 4) (F4)

DSC and ATR-FTIR assessment

The DSC peaks of pure ARB, CHT, and ARB-CHT-NP formulation 4 (F4) are shown in Fig. 2a and Table 2. The thermal analysis curves (Fig. 2a) indicate the disappearance of the ARB melting point in the CHT-NP, suggesting that ARB is in an amorphous form and is entrapped within the polymeric matrix of the nanoparticle. For ARB-CHT-NP, the CHT melting point appears, though with lower peak intensity, likely due to the lower amount of CHT in the NP compared to pure CHT. The functional groups in the molecular structure were characterized using ATR-FTIR spectroscopy to examine potential molecular interactions between ARB and the other components of the NP. The ATR-FTIR spectral profiles of ARB, CHT, and ARB-CHT-NP (F4) are shown in Fig. 2b and Table 2. It is important to note that no new chemical bonds or significant shifts in existing peaks were observed in the ATR-FTIR spectra, indicating no interactions between the functional groups of ARB and the other components of the NP. Like the DSC analysis, the ATR-FTIR spectra also confirm that ARB is entrapped in the CHT-NP.

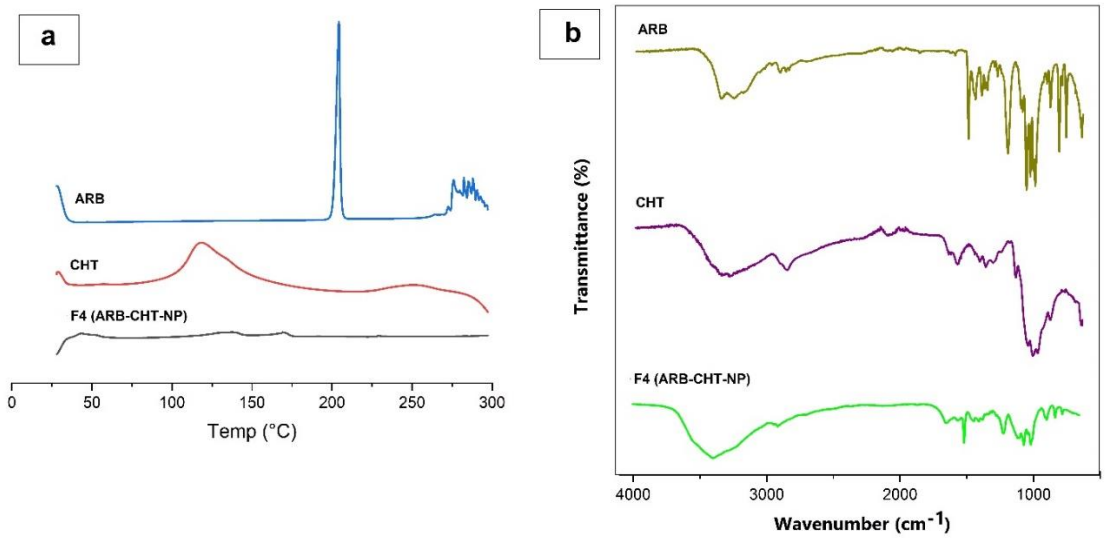

Fig. 2. DSC (a) traces and ATR-FTIR spectra (b) of ARB, CHT, and F4 (ARB-CHT-NP)

Table 2. ATR-FTIR and DSC data such as wavenumber, functional groups of components, and melting point.

Material	Wavenumber (cm^{-1})	Functional groups	Melting point
ARB	3400-3200	(O-H stretching)	208°C, sharp peak
	2920	(C-H stretching)	
	1510	(aromatic C=C stretching)	
	1215, 1076, 1011	C-O stretching	
CHT	3600–3100	(N–H and O–H stretching)	118°C
	2865	(C-H stretching))	
	1463-1457	(C-H bending)	
	1059, 1023	(C-O stretching).	

ARB release assay

The extended release of pharmaceutical agents from nanoparticles (NP) is crucial in determining drug bioavailability. This study investigated the release of ARB from ARB-CHT-NP gel (F4) and ARB-simple gel. The release profile is shown in Fig. 3. Compared to the ARB-simple gel, ARB-CHT-NP demonstrated a sustained release of ARB over 24 hours ($p < 0.05$).

On the other hand, the ARB-simple gel released ARB rapidly, with 72% released within the first 2 hours. ARB's in vitro release profile from CHT-NPs exhibited a two-stage release pattern (Figure 3). In the first stage, a rapid release of ARB was observed within the first 2 hours, with 30.313 ± 4.011% of ARB released. In the second stage (the controlled release phase), 60.837 ± 2.633% of the entrapped ARB was released over 24 hours. The initial rapid release of ARB can be attributed to weak adsorption or bonding of ARB to the surface of the NP. This loose binding leads to a burst release, as ARB readily dissolves upon contact with the release medium [28]. On the other hand, the polymeric NPs released ARB in a sustained manner. This can be attributed to the reduced rate of ARB diffusion from ARB-CHT-NP into the dissolution medium, likely due to the increased thickness of the CHT matrix [33]. Furthermore, the sustained release mechanism of chitosan nanoparticles is a complex process involving the interplay of diffusion, matrix swelling, and biodegradation. The intrinsic properties of chitosan, along with the external environment, influence the effectiveness of these parameters. The results confirm a controlled and prolonged drug release, which enhances therapeutic outcomes [34].

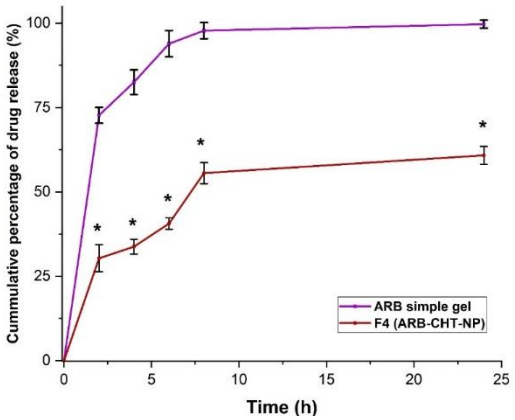

Fig. 3 Profile release of ARB from simple gel, and CHT-nanoparticle gel. ARB-CHT-NP releases ARB in a sustained release manner in comparison with ARR simple gel significantly. *($p<0.05$)

Previous studies have shown that the chitosan nanoparticles (CH-NP) of venlafaxine HCL (a hydrophilic drug) exhibited a lower release rate compared to the simple solution of venlafaxine HCL over 24 hours [19]. Similarly, the CHT/collagen-NP gel of kojic acid (a hydrophilic agent used for skin lightening) demonstrated a sustained release over 24 hours, in contrast to the simple kojic acid gel [35].

Ex vivo skin absorption

Figures 4 and 5 show that, for the studied formulations, including the ARB-CHT-NP and ARB simple gel, ARB crossed (Figure 4) and diffused (Figure 5) into the transdermal and dermal layers of rat skin, respectively. Superior skin transport was observed for the ARB-CHT-NP gel. The results demonstrated enhanced transdermal transfer for this formulation compared to the plain ARB gel ($p < 0.05$). The extent of ARB in the receiver compartment for the ARB-simple gel and ARB-CHT-NP gel was found to be 20.506 ± 3.668% (359.819 ± 64.375 µg/cm²) and 34.155 ± 2.699% (599.314 ± 47.371 µg/cm²), respectively ($p < 0.05$). These results indicate that ARB-CHT-NP gel had a higher transfer rate. Additionally, the extent of ARB deposited in the skin for ARB-CHT-NP gel and ARB gel was 46.168 ± 3.313% (810.094 ± 58.147 µg/cm²) and 19.881 ± 1.463% (348.847 ± 25.671 µg/cm²), respectively. Again, ARB-CHT-NP gel showed a higher deposition in the skin. These findings suggest that the CHT-NP gel is more advantageous than the conventional gel for specific local applications.

CHT-NPs offer a versatile and multifunctional approach to enhancing cosmetic products. Their ability to improve the delivery of active ingredients, enhance moisture retention, and provide controlled release properties makes them valuable additions to modern cosmetic formulations. Furthermore, due to their biocompatibility and biodegradability, CHT-NPs are well-suited for natural and sustainable cosmetic products [17].

CHT-NPs enhance skin absorption through two mechanisms: deep penetration via their nanoscale size, which allows passage through the stratum corneum, and improved adhesion to the skin due to their positive charge. These compounds are characterized by their ability to form a moisturizing film, increase permeability, and provide controlled and sustained release. By interacting with skin lipids, CHT-NPs create pathways that facilitate deeper penetration. Due to their excellent biocompatibility, CHT-NPs are safe and non-irritating, even for sensitive skin. Furthermore, their barrier function helps maintain skin health. Another key feature of these compounds is their ability to collectively improve the delivery and effectiveness of active ingredients in cosmetic products [17].

Previous studies have demonstrated that β-ARB-loaded CHT-NPs exhibited greater skin penetration at specific intervals. Additionally, it has been shown that CHT-NPs are a promising platform for the local administration of β-arbutin [36].

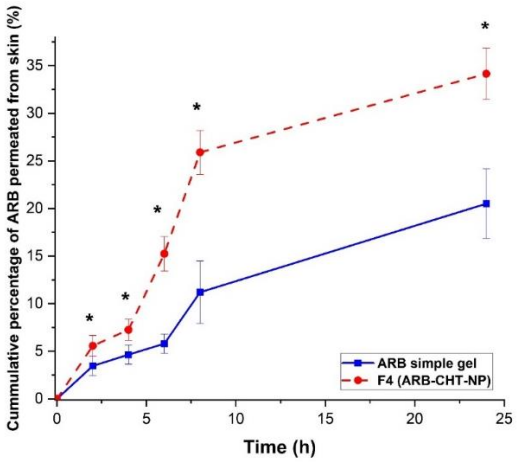

Fig. 4. The incremental extent of ARB simple gel and ARB-CHT-NP gel (F4) across animal cutaneous. *($p < 0.05$).

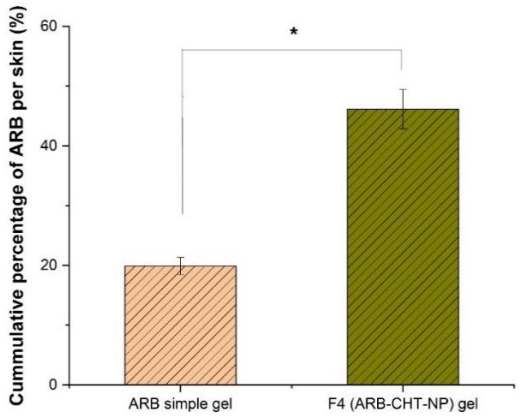

Fig. 5. Incremental level of ARB simple gel and ARB-CHT-NP gel (F4) deposited in animal cutaneous*($p < 0.05$).

MTT assay

The cytotoxicity of ARB, ARB-CHT-NP (F4), kojic acid, and blank CHT-NP (concentrations ranging from 50 to 1000 µM) was assessed on the HFF and B16F10 cell lines. As shown in Figures 6a and 6b, after treatment of the HFF cell line with ARB-CHT-NP (F4), kojic acid, and ARB, the percentage of surviving cells significantly declined over 24 and 48 hours ($p < 0.05$ and $p < 0.001$). After exposure to

ARB-CHT-NP (F4), ARB, and kojic acid for 24 and 48 hours, the percentage of surviving cells was as follows: (81% and 92%), (88% and 77%), and (83% and 71%), respectively. Similarly, treatment of the B16F10 cell line with ARB-CHT-NP (F4), ARB, and kojic acid resulted in a significant reduction in cell survival over 24 and 48 hours ($p < 0.001$) (Figures 6c and 6d). The percentage of surviving B16F10 cells after exposure to ARB-CHT-NP (F4), ARB, and kojic acid for 24 and 48 hours was as follows: (35% and 43%), (43% and 55%), and (42% and 51%), respectively. Furthermore, the IC50 values for ARB-CHT-NP (F4), ARB, and kojic acid on HFF normal fibroblast cells (after 24 and 48 hours of exposure) were (249.300 ± 10.400 µM and 56.600 ± 2.340 µM), (164.500 ± 7.65 µM and 49.92 ± 3.91 µM), and (210.000 ± 6.880 µM and 52.200 ± 4.170 µM), respectively. After 24 and 48 hours of exposure of the B16F10 cell line to ARB-CHT-NP (F4), ARB, and kojic acid, the IC50 values were (82.270 ± 7.340 µM and 78.100 ± 8.34 µM), (84.18 ± 9.23 µM and 108.100 ± 6.97 µM), and (119.000 ± 8.760 µM and 199.2 ± 8.12 µM), respectively. The optimal concentration for the melanin content assay was chosen based on the obtained IC50 values.

"Easy penetration of nanoparticles into cells can lead to cell death, making this one of the potential side effects of nanoparticle-based drug formulations. Oxidative stress is another key mechanism of cell death induced by nanoparticles. Due to the zeta potential surrounding NPs, their interaction with cells is enhanced, resulting in reduced cell viability in the presence of nanoparticles [37, 38]. Multiple mechanisms mediate the toxicity of CHT-NPs on B16F10 cells. These nanoparticles induce oxidative stress by generating reactive oxygen species (ROS), which damage cellular components and disrupt cellular function. Oxidative stress also triggers cell death through other pathways, including mitochondrial dysfunction, increased membrane permeability, impaired ATP production, and activation of apoptosis via intrinsic and extrinsic pathways. Additionally, previous studies have reported various mechanisms of CHT-NP-induced cell death, such as cell cycle arrest, interference with normal cell division, induction of an inflammatory response by releasing pro-inflammatory cytokines, lysosomal damage, release of harmful contents into the cytoplasm, and the promotion of oxidative stress [39-41].

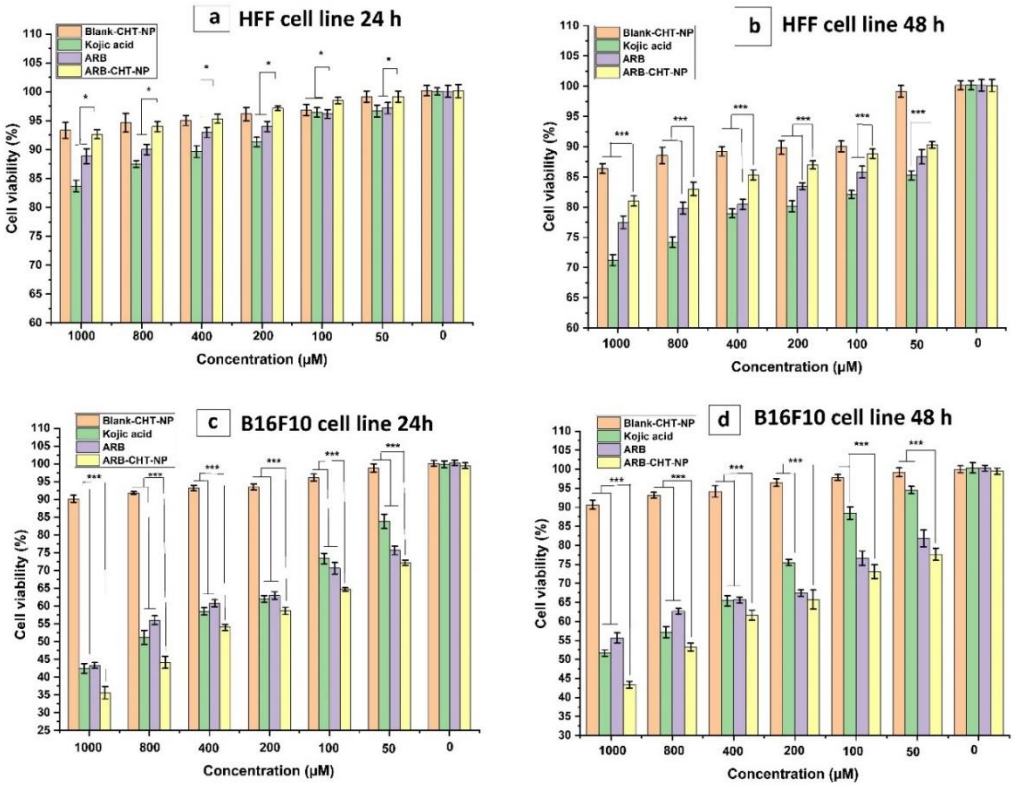

Fig. 6. Cytotoxicity effect of various preparations on HFF and B16F10 cell line. As shown in Figures 6a and 6b, over 24 and 48 hours, the cell survival of HFF normal fibroblast cells to test ARB-CHT-NP (F4), kojic acid, and ARB considerably declined *($p < 0.05$) ***($p<0.001$). As revealed in Fig 6c and 6d, using ARB-CHT-NP (F4), ARB and Kojic acid on B16F10 cells resulted in significant reductions in cell survival over 24 and 48 hours ***($p < 0.001$).

Melanin content results

The melanin content (intracellular melanin release) was examined in B16F10 cells after 24 and 48 hours of treatment. The IC50 values from the MTT assay were used to determine the optimal concentrations for the melanin content assay. The results showed that ARB-CHT-NP, ARB, and kojic acid inhibited melanin synthesis at 24 and 48 hours, while blank CHT-NP (at various concentrations) had no significant effect on melanin synthesis. After treatment of B16F10 cells with ARB-CHT-NP, ARB, and kojic acid (at their respective IC50 concentrations) for 24 hours, melanin content was significantly decreased in the spontaneous melanogenesis assay (Figure 7). The maximal inhibition observed for ARB-CHT-NP, ARB, and kojic acid was 58.739 ± 1.492%, 77.293 ± 1.123%, and 78.537 ± 1.598%, respectively, at concentrations of 83, 85, and 120 µM (Fig. 7a). As shown in Fig. 7a, ARB-CHT-NP was more effective than ARB, kojic acid, and blank CHT-NP in reducing melanin content during normal melanogenesis at 24 hours ($p < 0.001$). Furthermore, at 48 hours, ARB-CHT-NP (56.181 ± 2.208%) effectively inhibited melanin production compared to ARB (71.444 ± 2.288%) and kojic acid (74.741 ± 1.368%) ($p < 0.001$) (Fig. 7b). Additionally, Figure 8 schematically illustrates the mechanism of action of ARB as an inhibitor of the tyrosinase enzyme.

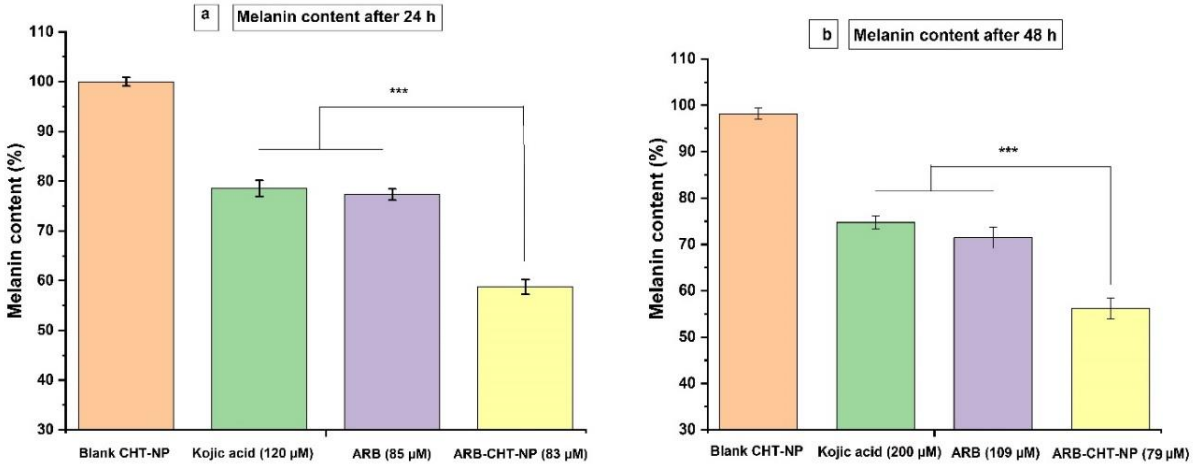

Fig. 7. Melanin content assay of various preparations in IC50 concentration. Fig 7a. The ARB-CHT-NP showed greater suppression of melanin content than either ARB and kojic acid or blank CHT-NP during normal melanin production at 24 h *** ($p<0.001$). Fig 7b. Also, ARB-CHT-NP exhibited a superior suppression of melanin content in comparison ARB and kojic acid during normal melanin production at 48 h (at 79, 109, and 200 µM) ***($p<0.001$).

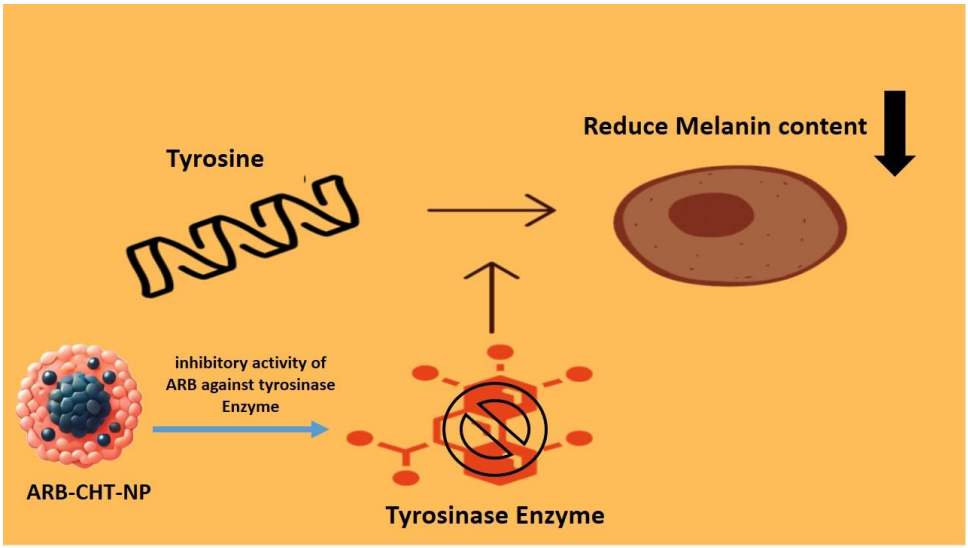

Fig. 8. Schematically mechanism illustration of action of ARB as an inhibitor of the tyrosinase enzyme

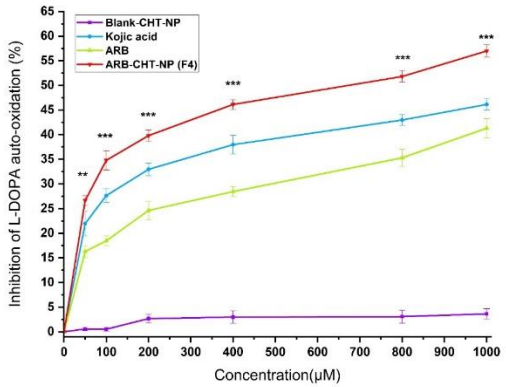

Fig.9. Effect of various preparations on the anti-oxidant influence of L-DOPA auto-oxidation. ARB-CHT-NP (F4) anti-oxidant influence on L-DOPA auto-oxidation was meaningfully upper than ARB and kojic acid *** ($p<0.001$).

ARB inhibits tyrosinase, the rate-limiting enzyme in the melanogenic pathway, thereby preventing melanin formation [42]. A promising strategy in cosmetic and dermatological applications is using CHT-NPs for the targeted delivery of ARB to melanocytes. This approach enhances the delivery and efficacy of ARB as a tyrosinase inhibitor while reducing potential side effects. As a result, it offers a promising solution for skin pigmentation disorders and achieving favorable skin-lightening effects. It can be concluded that ARB effectively reduces melanin production by specifically targeting tyrosinase and modulating melanogenic pathways. Additionally, ARB is a key ingredient in developing anti-melanogenic products. This study uses ARB-CHT-NP to provide a new, natural, and effective solution for managing skin hyperpigmentation issues. Therefore, significant advancements in skincare and dermatology are expected in subsequent studies [35].

Anti-oxidant effect of ARB-CHT-NP on L-DOPA

Skin hyperpigmentation significantly impacts the quality of life of patients, making effective anti-melanogenic products crucial [43]. This study demonstrated that all formulations, including ARB-CHT-NP (F4), ARB, and kojic acid, inhibited the oxidation of L-DOPA. As shown in Fig. 9, the maximum inhibitory levels for ARB and kojic acid solution (1000 µM) were 41.308 ± 1.967% and 46.141 ± 1.169%, respectively. The results indicate that increasing the ARB-CHT-NP (F4) concentration enhanced its antioxidant effect, with an inhibition of 56.971 ± 1.265%. Moreover, L-DOPA auto-oxidation was significantly inhibited by ARB-CHT-NP (F4) compared to ARB and kojic acid ($p < 0.001$).

ARB is known for its ability to scavenge free radicals and counteract oxidative stress, making it an effective antioxidant agent. This compound enhances auto-oxidation inhibition and is also a potent skin-lightening agent. The results suggest that incorporating ARB into hydrogels could offer significant benefits in cosmetic formulations [44].

Sensitivity assay on the dermis

Animal skin irritation tests are essential in nanotechnology to assess the' safety and potential risks of new nanomaterials. Nanomaterials with unique properties can interact with biological tissues, so evaluating their potential for adverse skin reactions in cosmetic products is essential. These tests are crucial in identifying and mitigating potential toxicological effects during the early stages of product development. In addition to meeting regulatory requirements, skin irritation tests guide product development, manage risks, and help manufacturers create safer products, ultimately ensuring consumer safety [45].

The influence of ARB formulations on dermal sensitivity, as assessed by edema and erythema ratings, is presented in Table 3. Compounds that receive a grade of 2 or lower are classified as non-irritants by Woodward, Draize, and Calvery, indicating that they do not cause skin irritation. The ARB-CHT-NP formulation demonstrated lower edema and erythema ratings (0.333) than other ARB and formalin formulations. Table 3 shows that the ARB-CHT-NP gel is suitable and safe for topical use, as it does not cause skin irritation.

Table 3. Cutaneous sensitivity values after local application.

	control		**ARB-CHT-NP gel**		**ARB-simple gel**		**blank CHT-NP gel**		**formalin**	
Rat num	Erythema	Edema	Erythema	Edema	Erythema	Edema	Erythema	Edema	Erythema	Edema
1	0	0	0	0	0	1	1	1	4	3
2	0	0	0	0	1	1	0	0	3	4
3	0	0	0	0	1	1	1	1	4	3
4	0	0	1	1	1	1	1	1	4	3
5	0	0	0	0	0	1	1	0	3	3
6	0	0	1	1	1	1	0	0	3	3

Animal skin irritation tests in pharmaceutical research are limited by differences between animal and human skin reactions, which can lead to inaccurate predictions of human responses. Ethical concerns and the logistical challenges of animal testing, such as time, cost, and delays in product development, further underscore the need for alternative methods. As a result, researchers are increasingly turning to human-derived tissues and cell cultures, such as reconstructed human epidermis models and in vitro assays, to provide more accurate predictions of human skin responses while promoting ethical and efficient research practices [46].

Limitation, challenge, suggestion, and future aspects

The study faced several limitations and challenges that may influence the interpretation and generalizability of its findings. One key limitation was the relatively small sample size, which could restrict the broader applicability of the results. Additionally, the evaluation period may not have been long enough to assess the long-term impacts of ARB-CHT-NP, highlighting the need for extended clinical trials to confirm its safety and efficacy in human subjects. Future research should employ advanced in vitro and in vivo assays to thoroughly investigate the molecular mechanisms underlying the anti-melanogenic effects, including the pathways involved in melanin synthesis inhibition and cellular uptake efficiency. Moreover, challenges associated with in vivo models, such as physiological differences between animal species and humans, could complicate the extrapolation of findings to human skin, emphasizing the need for tailored methodologies in future studies. Despite these challenges, the potential of CHT-NP products for skin lightening remains substantial. Future advancements should prioritize optimizing delivery systems, integrating natural and biocompatible constituents, implementing multi-targeted therapeutic strategies, and developing personalized solutions, all while ensuring compliance with regulatory standards. These efforts will drive the innovation of effective and safe skincare products that meet diverse consumer needs. Based on the findings of this study, ARB-CHT-NP shows considerable promise as a therapeutic option for addressing skin hyperpigmentation disorders, providing a solid foundation for further refinement and exploration in this emerging field.

CONCLUSION

This study incorporated ARB into CHT nanoparticles made from a natural polymer. The investigations showed that ARB within the CHT nanoparticles was in an amorphous phase, and no molecular interactions with other components of the nanoparticles were observed. The mean loading efficiency, PDI, NP diameter, and zeta potential (ZP) for ARB-loaded CHT nanoparticles were 97.151 ± 0.066%, 0.209 ± 0.007, 215.666 ± 5.976 nm, and 11.466 ± 0.986 mV, respectively. The cutaneous diffusion experiment demonstrated that the extent of ARB in the dermal layers (in the receptor compartment) was higher for the ARB-CHT-NP gel than the ARB simple gel. Additionally, for the optimal ARB-CHT-NP formulation, cellular viability was about 81% and 92% after 24 and 48 hours, respectively. The MTT assay revealed lower toxicity in HFF cells than in other treated cells. Furthermore, the optimal ARB-CHT-NP formulation showed more cytotoxic effects on melanoma cancer cells (B16F10 cell line) than kojic acid and the ARB solution. Furthermore, the safety of ARB-CHT-NP gel was confirmed in a cutaneous sensitivity assay. ARB-CHT-NP exhibited the most excellent anti-pigmentation effect, including reduced melanin production and inhibition of L-DOPA auto-oxidation, outperforming intact ARB, kojic acid, and drug-free CHT-NP. This study highlights the potential of ARB-CHT-NP gel as a depigmenting agent, suggesting its suitability for integration into both pharmaceutical and cosmetic markets. Biocompatible nanoparticles, such as ARB-CHT-NP gel, present a groundbreaking opportunity to transform the cosmetic industry by enabling site-specific delivery of active compounds, maximizing their absorption, and therapeutic benefits. Despite these promising preliminary results, further research is needed to rigorously assess the safety and efficacy of these substances in cosmeceutical applications and to refine their production processes to ensure scalability and economic viability.

ACKNOWLEDGMENT

The authors sincerely thank the Research Council of Hormozgan University of Medical Sciences, Bandar Abbas, Iran, for their valuable technical cooperation. This study was funded by grant number [4020099] from Hormozgan University of Medical Sciences, Bandar Abbas, Iran. The authors declare that no potential conflicts of interest were reported.

DISCLOSURE STATEMENT

The authors reported no potential conflict of interest.

FUNDING

This study was funded by a grant number [4020099] from the Hormozgan University of Medical Sciences, Bandar Abbas, Iran.

ETHICAL APPROVAL

As part of the present study, all animal experiments were approved by the Ethical Committee for Animal Investigation at HUMS with the code of IR.HUMS.REC.1402.223. All animal experiments followed ARRIVE protocols (Animal Research: Reporting of *in vivo* Experiments) and were conducted under the UK Animals (Scientific Procedures) Act 1986 and EU Directive 2010/63/EU on animal experimentation.

DATA AVAILABILITY STATEMENT

All datasets generated for this study are included in the article.

REFERENCES

1. Picardi A, Abeni D, Melchi C, Puddu P, Pasquini P. Psychiatric morbidity in dermatological outpatients: an issue to be recognized. Br J Dermatol. 2000;143(5):983-991.
2. Deshpande SS, Khatu SS, Pardeshi GS, Gokhale NR. Cross-sectional study of psychiatric morbidity in patients with melasma. Indian J Psychiatry. 2018;60(3):324-328.
3. Rendon M, Berneburg M, Arellano I, Picardo M. Treatment of melasma. J Am Acad Dermatol. 2006;54(5):S272-S281.
4. Levy LL, Emer JJ. Emotional benefit of cosmetic camouflage in the treatment of facial skin conditions: personal experience and review. Clin Cosmet Investig Dermatol. 2012:173-182.
5. Sheth VM, Pandya AG. Melasma: a comprehensive update: part II. J Am Acad Dermatol. 2011;65(4):699-714.
6. Clardy J, Walsh C. Lessons from natural molecules. Nature. 2004;432(7019):829-837.
7. Zhu W, Gao J, editors. The use of botanical extracts as topical skin-lightening agents for the improvement of skin pigmentation disorders. J Investig Dermatol Symp Proc; 2008: Elsevier.
8. Inoue Y, Hasegawa S, Yamada T, Date Y, Mizutani H, Nakata S, et al. Analysis of the effects of hydroquinone and arbutin on the differentiation of melanocytes. Biol Pharm Bull. 2013;36(11):1722-30.
9. Tada M, Kohno M, Niwano Y. Alleviation effect of arbutin on oxidative stress generated through tyrosinase reaction with L-tyrosine and L-DOPA. BMC Biochem. 2014;15:1-7.
10. Ertam I, Mutlu B, Unal I, Alper S, Kivcak B, Ozer O. Efficiency of ellagic acid and arbutin in melasma: A randomized, prospective, open-label study. J Dermatol. 2008;35(9):570-574.
11. Polnikorn N. Treatment of refractory melasma with the MedLite C6 Q-switched Nd: YAG laser and alpha arbutin: a prospective study. J Cosmet Laser Ther. 2010;12(3):126-131.
12. Davis EC, Callender VD. Postinflammatory hyperpigmentation: a review of the epidemiology, clinical features, and treatment options in skin of color. J Clin Aesthet Dermato. 2010;3(7):20.
13. Fong P, Tong HH. In silico prediction of the cosmetic whitening effects of naturally occurring lead compounds. Nat Prod Commun. 2012;7(10):1934578X1200701010.
14. Khezri K, Saeedi M, Morteza-Semnani K, Akbari J, Rostamkalaei SS. An emerging technology in lipid research for targeting hydrophilic drugs to the skin in the treatment of hyperpigmentation disorders: kojic acid-solid lipid nanoparticles. Artif Cells Nanomed Biotechnol. 2020;48(1):841-853.
15. Sharma V, Anandhakumar S, Sasidharan M. Self-degrading niosomes for encapsulation of hydrophilic and hydrophobic drugs: an efficient carrier for cancer multi-drug delivery. Mater Sci Eng C. 2015;56:393-400.
16. Mohammadian E, Rahimpour E, Alizadeh-Sani M, Foroumadi A, Jouyban A. An overview on terbium sensitized based-optical sensors/nanosensors for determination of pharmaceuticals. Appl Spectrosc Rev. 2022;57(1):39-76.
17. Ta Q, Ting J, Harwood S, Browning N, Simm A, Ross K, et al. Chitosan nanoparticles for enhancing drugs and cosmetic components penetration through the skin. Eur J Pharm Sci. 2021;160:105765.
18. Shah S, Pal A, Kaushik V, Devi S. Preparation and characterization of venlafaxine hydrochloride-loaded chitosan nanoparticles and in vitro release of drug. J Appl Polym Sci. 2009;112(5):2876-2887.
19. Saeedi M, Morteza-Semnani K, Siahposht-Khachaki A, Akbari J, Valizadeh M, Sanaee A, et al. Passive targeted drug delivery of venlafaxine hcl to the brain by modified chitosan nanoparticles: Characterization, cellular safety assessment, and in vivo evaluation. J Pharm Innov. 2023;18(3):1441-1453.
20. Nawaz A, Wong TW. Chitosan-carboxymethyl-5-fluorouracil-folate conjugate particles: microwave modulated uptake by skin and melanoma cells. J Invest Dermatol. 2018;138(11):2412-2422.
21. Haque S, Md S, Fazil M, Kumar M, Sahni JK, Ali J, et al. Venlafaxine loaded chitosan NPs for brain targeting: pharmacokinetic and pharmacodynamic evaluation. Carbohydr Polym. 2012;89(1):72-79.
22. Calvo P, Remunan-Lopez C, Vila-Jato JL, Alonso M. Novel hydrophilic chitosan-polyethylene oxide nanoparticles as protein carriers. J Appl Polym Sci. 1997;63(1):125-132.
23. Hashemi SMH, Enayatifard R, Akbari J, Saeedi M, Seyedabadi M, Morteza-Semnani K, et al. Venlafaxine HCl encapsulated in niosome: green and eco-friendly formulation for the management of pain. AAPS Pharm Sci Tech. 2022;23(5):149.
24. Saeedi M, Morteza-Semnani K, Akbari J, Rahimnia SM, Babaei A, Eghbali M, et al. Eco-friendly preparation, characterization, evaluation of anti-melanogenesis/antioxidant effect and in vitro/in vivo safety profile of kojic acid loaded niosome as skin

lightener preparation. J Biomater Sci Polym Ed. 2023;34(14):1952-1980.
25. Gatabi ZR, Saeedi M, Morteza-Semnani K, Rahimnia SM, Yazdian-Robati R, Hashemi SMH. Green preparation, characterization, evaluation of anti-melanogenesis effect and in vitro/in vivo safety profile of kojic acid hydrogel as skin lightener formulation. J Biomater Sci Polym Ed. 2022;33(17):2270-2291.
26. Masarudin MJ, Cutts SM, Evison BJ, Phillips DR, Pigram PJ. Factors determining the stability, size distribution, and cellular accumulation of small, monodisperse chitosan nanoparticles as candidate vectors for anticancer drug delivery: application to the passive encapsulation of [14C]-doxorubicin. Nanotechnol Sci Appl. 2015:67-80.
27. Hejjaji EM, Smith AM, Morris GA. Evaluation of the mucoadhesive properties of chitosan nanoparticles prepared using different chitosan to tripolyphosphate (CS: TPP) ratios. Int J Biol Macromol. 2018;120:1610-1617.
28. Abd El-Aziz BA. Improvement of kojic acid production by a mutant strain of Aspergillus flavus. J Nat Sci Res. 2013;3(4):31-41.
29. Pant A, Negi JS. Novel controlled ionic gelation strategy for chitosan nanoparticles preparation using TPP-β-CD inclusion complex. Eur J Pharm Sci. 2018;112:180-185.
30. Pan C, Qian J, Zhao C, Yang H, Zhao X, Guo H. Study on the relationship between crosslinking degree and properties of TPP crosslinked chitosan nanoparticles. Carbohydr Polym. 2020;241:116349.
31. Al-Nemrawi N, Alsharif S, Dave R. Preparation of chitosan-TPP nanoparticles: the influence of chitosan polymeric properties and formulation variables. Int J Appl Pharm. 2018;10(5):60-65.
32. Akbari J, Saeedi M, Morteza-Semnani K, Hashemi SMH, Babaei A, Eghbali M, et al. Innovative topical niosomal gel formulation containing diclofenac sodium (niofenac). J Drug Target. 2022;30(1):108-117.
33. Maji R, Ray S, Das B, Nayak AK. Ethyl cellulose microparticles containing metformin HCl by emulsification-solvent evaporation technique: effect of formulation variables. Int Sch Res Notices 2012;2012.
34. Raju G, Mas Haris MRH, Azura A, Ahmed Mohamed Eid AM. Chitosan epoxidized natural rubber biocomposites for sorption and biodegradability studies. ACS Omega. 2020;5(44):28760-28766.
35. Saeedi M, Morteza-Semnani K, Akbari J, Rahimnia SM, Ahmadi F, Choubdari H, et al. Development of kojic acid loaded collagen-chitosan nanoparticle as skin lightener product: in vitro and in vivo assessment. J Biomater Sci Polym Ed. 2024;35(1):63-84.
36. Sahudin S, Sahrum Ayumi N, Kaharudin N. Enhancement of skin permeation and penetration of β-arbutin fabricated in chitosan nanoparticles as the delivery system. Cosmetics. 2022;9(6):114.
37. Akbari J, Saeedi M, Enayatifard R, Morteza-Semnani K, Hashemi SMH, Babaei A, et al. Curcumin Niosomes (curcusomes) as an alternative to conventional vehicles: A potential for efficient dermal delivery. J Drug Deliv Technol. 2020;60:102035.
38. Liu P, Boyle AJ, Lu Y, Adams J, Chi Y, Reilly RM, et al. Metal-chelating polymers (MCPs) with zwitterionic pendant groups complexed to trastuzumab exhibit decreased liver accumulation compared to polyanionic MCP immunoconjugates. Biomacromolecules. 2015;16(11):3613-3623.
39. Miyayama T, Matsuoka M. Involvement of lysosomal dysfunction in silver nanoparticle-induced cellular damage in A549 human lung alveolar epithelial cells. J occup med toxicol. 2016;11:1-6.
40. Zubareva A, Svirshchevskaya E. Mechanisms of the interaction of chitosan and its derivatives with the cell. Prikl Biokhim Mikrobiol. 2016;52(5):448-454.
41. Mohammadian E, Foroumadi A, Hasanvand Z, Rahimpour E, Zhao H, Jouyban A. Simulation of mesalazine solubility in the binary solvents at various temperatures. J Mol Liq. 2022;357:119160.
42. Rudeekulthamrong P, Kaulpiboon J. Optimization of amylomaltase for the synthesis of α-arbutin derivatives as tyrosinase inhibitors. Carbohydr Res. 2020;494:108078.
43. Rigopoulos D, Gregoriou S, Katsambas A. Hyperpigmentation and melasma. Cosmet Dermatol. 2007;6(3):195-202.
44. Dastan Z, Pouramir M, Ghasemi-Kasman M, Ghasemzadeh Z, Dadgar M, Gol M, et al. Arbutin reduces cognitive deficit and oxidative stress in animal model of Alzheimer's disease. Int J Neurosci. 2019;129(11):1145-1153.
45. Fytianos G, Rahdar A, Kyzas GZ. Nanomaterials in cosmetics: Recent updates. Nanomaterials. 2020;10(5):979.
46. Nakamura M, Haarmann-Stemmann T, Krutmann J, Morita A. Alternative test models for skin ageing research. Exp Dermatol. 2018;27(5):495-500.